J Plant Growth Regul (2010) 29:232–241
DOI 10.1007/s00344-009-9127-2

Blue Light Exposure Targets NADPH Oxidase to Plasma Membrane and Nucleus in Wheat Coleoptiles

Kumar Chandrakuntal · Ashish K. Shah · Neena M. Thomas · V. Karthika · Malini Laloraya · Pradeep G. Kumar · Manmohan M. Laloraya

Received: 20 August 2009 / Accepted: 18 November 2009 / Published online: 11 December 2009

Abstract Wheat coleoptile tips generate superoxide radical as a part of the phototropic response to blue light, but the source of this free radical generation is not known. We evaluated the presence and involvement of homologs of neutrophil NADPH oxidase (NOX), including gp91phox, p22phox, p67phox, p47phox, and p40phox, in wheat coleoptiles using Western blot analysis and immunofluorescence microscopy. Blue light augmented the expression levels of all these subunits and targeted NOX subunits onto the plasma membrane and to the nucleus. gp91phox, p22phox, p67phox, and p40phox showed entry into the nucleus and exhibited physical closeness with DNA. CuZnSOD was also present in the coleoptile tip, which also showed a blue-light-dependent elevation in expression. Superoxide production and phototropic response were both abrogated by DPIC and staurosporine, indicating their cause-and-effect relationship. We conclude that blue light mediates a phototropic response in wheat coleoptiles through modulation of expression of NOX and SOD as well as the translocation of NOX subunits onto the plasma membrane and nuclear membrane. Thus, this study provides a mechanistic explanation for superoxide production during the photoresponse in wheat coleoptiles.

Keywords Coleoptile · Blue light · Superoxide · Signal transduction NOX

K. Chandrakuntal · A. K. Shah · N. M. Thomas · V. Karthika · M. Laloraya · P. G. Kumar (✉) · M. M. Laloraya
Rajiv Gandhi Centre for Biotechnology, Thycaud, PO, Poojappura, Thiruvananthapuram, Kerala 695 014, India
e-mail: kumarp@rgcb.res.in

Introduction

Plants perceive blue light through FAD-based cryptochromes (CRY1/2) or FMN-based phototropins (PHOT1/2). Though they both regulate various functions in plants, the initial photochemistry underlying their function is not known. An immediate reaction at the receptor level appears to be its phosphorylation as is shown in the case of CRY1 (Shalitin and others 2003) and CRY2 (Shalitin and others 2002) through their autokinase activity (Briggs and others 2001; Ozgur and Sancar 2006). Blue light excitation has been shown to generate neutral flavin radicals within the cryptochrome (Immeln and others 2007) and phototropin (Kay and others 2003). We reported that blue light excitation of the wheat (*Triticum vulgare*) coleoptile tip triggered a reactive oxygen species (ROS) burst (Laloraya and others 1999; Chandrakuntal and others 2004) through a tightly coupled system that produces hydrogen peroxide (H_2O_2) (Chandrakuntal and others 2004). A role for H_2O_2 has been invoked in various signalling events, in both plants and animals (Bedard and others 2007; Brown and Griendling 2009). In plants, the role of ROS has been associated with physiological events, including phototropic curvature (Chandrakuntal and others 2004), cell growth (Foreman and others 2003), and in hypersensitive responses (Tenhaken and others 1995).

Enzymatic production of superoxide ($O_2^{\cdot-}$) depends largely on a family of NADPH oxidases (Nox) and that of its immediate downstream product H_2O_2 on superoxide dismutase (SOD) and dual oxidases (Duox) (Bedard and others 2007; Brown and Griendling 2009). Nox1-5 and Duox1/2 are recognized as the key molecules involved in the one-electron reduction of molecular oxygen. Nox1-4 have two membrane-bound subunits (a catalytic subunit

known as the gp91phox homolog and a regulatory subunit known as p22phox). Nox1-3 have several cytosolic regulatory subunits, whereas Nox4 does not have any identified regulatory molecule of this category. Nox-5 possesses cytoplasmic EF hands and is calcium-modulated. A detailed review of the structural aspects of these proteins has appeared recently (Brown and Griendling 2009).

The neutrophil Nox (formerly known as the phagocyte oxidase Phox) is the major source of ROS in the vasculature (Bokoch 1994) and has the best worked out structural detail available today. It consists of a catalytic subunit (Nox1, Nox2, Nox3, Nox4, or Nox5), p22phox, p47phox, p67phox, and the small guanosine triphosphatase Rac1. Genes encoding homologs of the gp91(phox) subunit of the plasma membrane NADPH oxidase (NOX) complex are thought to be a source of ROS during the oxidative burst (Auh and Murphy 1995; Desikan and others 1996) which is part of the defence response (Desikan and others 1996; Sagi and Fluhr 2001). The involvement of a plasma membrane-associated NOX in the oxidative burst in plants was speculated (Apostol and others 1989) and could be reminiscent of the oxidative burst during activation of mammalian neutrophils (Taylor and others 1993; Keller and others 1998). The targeting of NOX to focal complexes in lamellipodia and membrane ruffles through the interaction of p47phox with the scaffold proteins TRAF4 and WAVE1 provides a mechanism for achieving localized ROS production (Ushio-Fukai 2006).

The neutrophil NOX homolog in *Arabidopsis* appears to be a plasma membrane-located 108-kDa protein, with a C-terminal region that shows pronounced similarity to the 69-kDa apoprotein of the gp91phox subunit and is regulated by both Ca^{2+} and G protein stimulation (Keller and others 1998). The plant homolog of NOX can produce $O_2^{\cdot-}$ in the absence of additional cytosolic components and is stimulated directly by Ca^{2+} (Sagi and Fluhr 2001). Plants that demonstrated a phototropic bending response also demonstrated Ca^{2+} influx into the light side approximately 20 min after the start of blue light exposure (Babourina and others 2004), which also suggested that the blue light-induced signal transduction cascade might not be dependent on cytosolic subunits of NOX.

In this context, we examined the presence of homologs of the catalytic and regulatory components of neutrophil NOX in wheat coleoptiles. We also conducted experiments addressing the mechanistic aspects of blue-light-mediated ROS production in terms of dynamics and expression of NOX subunits in wheat coleoptile tips.

Materials and Methods

Reagents

Staurosporine, riboflavin, diphenylene iodonium chloride (DPIC), ethylenediamine tetraacetic acid (EDTA), *N-tert*-butyl-α-phenyl nitrone (PBN), and 3-[(3-cholamidopropyl) dimethylammonio]-1-propanesulfonate (CHAPS), paraformaldehyde (PFA), NADPH, and propidium iodide (PI) were purchased from Sigma Chemical Co. (St. Louis, MO, USA). Goat anti-rabbit IgG-HRP, goat anti-rabbit IgG-FITC, and rabbit polyclonal antibodies to gp91phox (H-60), p22phox (FL-125), p67phox (H-300), p47phox (H-195), p40phox (H-300), actin (H-196), CuZnSOD, and MnSOD were purchased from Santa Cruz Biotechnology Inc. (Santa Cruz, CA, USA); NaK-ATPase (mouse monoclonal) from Abcam (Cambridge, UK); diaminobenzidine dihydrochloride (DAB) from Merck (Darmstadt, Germany); diethyl dithio carbamic acid (DDC), Triton X-100, and polyvinylene difluoride (PVDF) membranes (0.45μ Sequiblot) from Bio-Rad Laboratory (Hercules, CA, USA); fluorescein diacetate (FDA) from Molecular Probes® (Invitrogen, Carlsbad, CA, USA); nitroblue tetrazolium and 5-bromo-4-chloro-3-indolyl phosphate from Zymed (San Francisco, CA, USA); phenyl methyl sulphonyl fluoride (PMSF) and *N*,*N*,*N*′,*N*-tetremethyl ethylene diamine (TEMED) from Lancaster Synthesis (Morecambe, UK); all other chemicals were from HiMedia Laboratories, India.

Western Blotting

Dark-grown coleoptile tips were exposed to blue light (450 nm, 3 mW/m^2) for 15 min using a Ace 150-W cold light fiber optic illuminator (Schott, Elmsford, NY, USA), after which they were kept in the dark for 2 h. Protein extracts were made from the extreme 3-mm tips of coleoptiles from blue-light-exposed and dark control groups. 1000 copeoptile tips were homogenized in 1 ml phosphate buffer (pH 7.2) at 13,000 rpm (Polytron, Switzerland) and the homogenate was centrifuged for 30 min at 14,000 *g* at 4°C. The supernatant was collected as the cytosolic fraction. The pellets were resuspended in 100 µl of Triton X buffer (2% Triton X-100, 0.05% PMSF, 0.08% sodium orthovanadate, and 0.04% EDTA in PBS). After sonication at 20 kHz (3 cycles, 30 s each), the suspension was incubated on ice for 30 min and centrifuged at 14,000 *g* at 4°C for 40 min. The supernatant was collected as the Triton-soluble fraction. These pellets were resuspended in membrane solubilization buffer (0.5 M Tris HCl, pH 6.8; 10% SDS; 0.05% CHAPS). The suspension was sonicated and centrifuged at 14,000 *g* at 4°C for 40 min. The supernatant

thus obtained was collected as the SDS-soluble fraction. The protein concentration in each of the fractions was estimated using DC Protein Assay Reagent (Bio-Rad, Gurgaon, India), and the final concentration was adjusted to 1 μg/μl. The protein extracts (10 μg/well) were electrophoresed on 12% SDS–polyacrylamide gels and were electrophoretically transferred (35 mA, 16 h) onto PVDF membrane equilibrated in transfer buffer [25 mM Tris, 190 mM glycine (pH 8.2), 40% methanol (v/v)]. After transfer, the membranes were blocked in 5% nonfat dry milk for 2 h and incubated for 2 h with an appropriate dilution of primary antibodies prepared in PBST. After thorough washing with PBST, they were incubated for 1 h in goat anti-rabbit IgG HRP (1:2000) prepared in PBST. The membranes were washed three times with PBST, developed using DAB, dried, and imaged on a Bio-Rad imager. The band intensities were computed using Phoretix (version 2.0, Nonlinear Dynamics, Newcastle upon Tyne, UK) and baseline corrections were applied. The computed band intensities from five independent replicates for each of the experiments were pooled and mean ± standard error was calculated. The data were subjected to analysis of variance (SPSS v10.0, SPSS Inc., Chicago, IL, USA).

Confocal Microscopy

Coleoptile tips (dark- and blue-light-treated) were sectioned longitudinally and snap-fixed in 4% PFA. PFA-fixed sections were neutralized with 50 mM NH_4Cl and permeabilized with 0.25% Triton X-100. Treated sections were blocked with 5% milk for 2 h and were incubated with anti-phox primary antibodies. The sections were thoroughly washed and probed with goat anti-rabbit IgG-FITC. Propidium iodide was used for nuclear staining. The sections were mounted on glass slides and imaged on a Leica TCS SP2 AOBS confocal laser scan microscope (Leica, Germany). FITC emission was gathered using 488-nm laser excitation and the emission was collected at 535 nm. PI emission was gathered using 530-nm excitation and 660-nm emission. Signals were gathered in the sequential mode. For fluorescence resonance energy transfer measurement, the specimens were excited with 488 nm and emission at 660 nm was captured to determine the energy exchange between FITC and PI.

NADPH Oxidase Activity

For each experiment, 100 coleoptiles were selected and four segments (0–2, 2–4, 4–6, and 6–8 mm) were excised and subjected to subsequent experimentation. The coleoptile segments were homogenized in 1 ml phosphate buffer (pH 7.2) at 13,000 rpm (Polytron, Switzerland) at 4°C, and the homogenates were clarified by centrifuging at 5000*g*. The supernatant was collected for the NOX activity assays. For this, 750 μl of the supernatant was mixed with 2.25 ml of phosphate buffer containing 10 mM NADPH. The control preparation received no added NADPH.

Coleoptile homogenates, prepared as mentioned above, were aliquoted into 80-μl fractions in separate glass tubes. Each fraction was mixed with 9 μl fresh phosphate buffered saline (PBS), 1 μl DDC (1 M) and 10 μl PBN (500 mM). The reaction mixtures were vortexed gently and incubated in the dark for 1 h after the introduction of PBN. After the incubation, a 25-μl aliquot was loaded into a quartz capillary tube and ESR spectra were recorded on an X-band ESR spectrometer (Varian E-104 with TM-110 cavity). For each experiment, two identical preparations were made, of which one sample was exposed to blue light (450 ± 10 nm, 15-min exposure at 3 mW/m^2) using an Ace 150-W cold light fiber optic illuminator (Schott) and the second tube served as a dark control.

To evaluate the role of NADPH oxidase inhibitors, the selected inhibitor was incorporated into the homogenate (in 9-μl volume) to give a 10-μM final concentration and incubated for 45 min prior to the addition of PBN.

All the ESR spectra were recorded at room temperature under the following settings: scan range, 100 G; field set, 3237 G; time constant, 1 s; scan time, 4 min; modulation amplitude, 2 G; modulation frequency, 100 kHz; and receiver gain, 2.5×10^5. Line intensities of PBN-O_2^- adducts were computed based on the spectral properties ($a^N = 1.48$ mT and $a^H\beta = 0.198$ mT). The experiments were repeated five times with fresh samples and the mean ± standard deviation was computed. The data were subjected to analysis of variance using SPSS v10.

Histochemical Assay for SOD Activity

Coleoptile sections were treated with 2 mM nitroblue tetrazolium (NBT) for 30 min. They were later incubated in a solution containing 0.036 M potassium phosphate (pH 7.8), 0.028 M tetramethyl ethylene diamine, and 2.8×10^{-5} M riboflavin for 30 min. The sections were then illuminated for 30 min by a 15-W fluorescent lamp. Control sections were incubated in the same medium supplemented with 1 mM DDC as an inhibitor of Cu–Zn SOD. The sections were rinsed in 0.036 M phosphate buffer (pH 7.8), mounted in glycerol jelly, and observed under a Nikon-Optiphot microscope under phase contrast optics. Photographs were taken on a Nikon F-301 camera.

Detection of AOS in Wheat Coleoptile Tip

Approximately 1000 seeds of *Triticum vulgare* were germinated in a temperature-controlled (25 ± 1°C) dark room. The coleoptile tips (approximately 1 cm long) were

excised on day 5 under green light (535-nm green interference filter, Nikon). The tips were sectioned longitudinally (approximately 50 μM) through the apex and the sections were placed on a glass slide. FDA fluorescence was measured after treating the coleoptiles in a solution of 3 μM FDA for 2 min. The ability to focus on the specimen was enabled under UV epi-illumination using a UV 1-A (DM 400) Nikon filter in total darkness. The extreme apex of the coleoptile tip was illuminated with a narrow spot of blue light for 1 min using a Nikon B-2A (450 nm) filter in total darkness under safe red light. Simultaneously, exposures were taken through a camera port fitted with a Nikon F-301 camera.

To evaluate the effect of NADPH oxidase inhibitor on FDA fluorescence, coleoptile tips were incubated with 10 μM final concentration of DPIC for 30 min prior to incubation with FDA. Control incubation was performed in PBS without any selected NADPH oxidase inhibitors.

Phototropic Curvature Experiments

Dark-grown coleoptile tips with shoot lengths of 5 cm were selected and divided into four groups of ten coleoptiles each. Group 1 served as the dark control. Group 2 coleoptiles were unilaterally exposed to blue light (450 nm, 3 mW/m^2) for 2 h using an Ace 150-W cold light fiber optic illuminator (Schott). Groups 3 and 4 coleoptiles were immersed for 15 min in DPIC (10 μM) and staurosporine (100 nM), respectively, before they were exposed to blue light as mentioned above. The coleoptiles were photographed and the degree of curvature was measured.

Results

Western Blot Analysis of NOX Components

Our Western blot results indicated that gp91phox was enriched in the Triton X-100- and SDS-sensitive membrane compartments (Fig. 1a, lanes 3–6), whereas the cytosolic fraction was characterized by the absence of this protein. There was no significant change in the localization or expression of gp91phox following blue light exposure (Fig. 1a, lanes 1, 2). However, there was a significant upregulation of p22phox in the cytosolic fraction (Fig. 1b, lane 2), though Triton X-100- and SDS-sensitive fractions of p22 did not show significant alterations in response to blue light. Blue light exposure of coleoptiles brought about significant enhancement in the expression of the regulatory NOX components p67phox, p47phox, and p40phox in various compartments. p67phox partitioned strongly into the Triton-insensitive and SDS-sensitive compartments, whereas p47phox and p40phox incorporated into both Triton-sensitive and SDS-sensitive compartments. A 20-fold increase of p67phox was observed in the cytosolic fractions (Fig. 1c, lanes 1, 2), whereas p47phox showed a greater accumulation in the cytosolic (Fig. 1d, lanes 1, 2) and Triton-soluble fractions (Fig. 1d, lanes 3, 4). p40phox showed significant accumulation in the Triton X-100- and SDS-sensitive compartments in blue-light-exposed coleoptiles (Fig. 1e, lanes 1–6). Densitometric quantitation of band intensities from five replicates of each of the experiments is presented as a bar diagram on the right-hand side of each of the blots.

Immunofluorescence Analysis of NOX Distribution

In etiolated coleoptiles, gp91phox localized predominantly on the cell membrane (marked by white arrows in Fig. 2), and a mesh-like distribution in the cytoplasm (marked by asterisk), typical of cytoskeleton-associated proteins, was also evident. Surprisingly, we observed the presence of green fluorescence within the nucleus, indicating the nuclear localization of gp91phox as well (Fig. 2Aa–Ac). The distribution of p22phox was similar to that of gp91phox (Fig. 2Ba–Bc). Excitation with blue light brought about a significant increase in the localization of p22phox on the plasma membrane and in the cytosol (Fig. 2Ba and Bd, Bc and Bf).

The expression of p67phox in apical cells of etiolated coleoptiles was moderate and restricted mainly to the plasma membrane in some scattered and speckled distribution within the cytoplasm (Fig. 2Ca, Cc). The nuclei of these cells also were stained with p67phox antibody (Fig. 2Cc). After exposure to blue light, the expression of p67phox showed visible enhancement within the cytoplasm, and the plasma membrane association of this molecule was also augmented (Fig. 2Cd, Cf). The localization of p67phox within the nucleus was evident (Fig. 2Cd). p47phox showed heavy localization within the apical cells, making it difficult to resolve the plasma membrane localization, if any, of this molecule (Fig. 2Da, Dc). In contrast to the other phox subunits mentioned in the previous section, p47phox did not show preferential localization in the nucleus (Fig. 2Dc). Blue light exposure of the coleoptile tip brought about heavy accumulation of p47phox onto the plasma membrane (Fig. 2Dd, Df). Further, p40phox did not accumulate in the nuclei of apical cells in either etiolated (Fig. 2Dc) or blue-light-exposed (Fig. 2Df) coleoptiles.

p40phox was present in the cytosol, plasma membrane, and nuclei of etiolated cells (Fig. 2Ea, Ec). Exposure to blue light brought about a quantitative increase in the

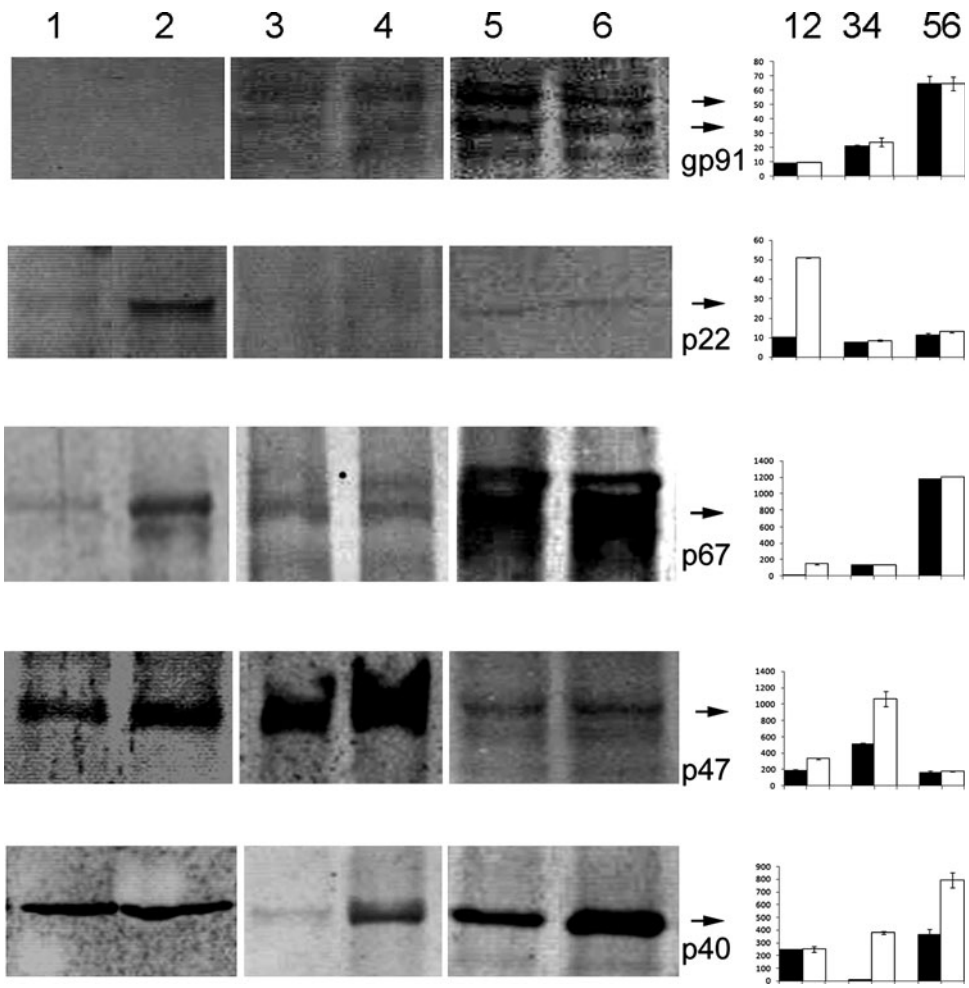

Fig. 1 Characterization and localization of NOX components. Western blots of cytosolic, Triton-soluble, and SDS-soluble protein extracts from wheat coleoptile tip probed with various NOX antibodies. Lanes with odd numbers represent dark controls and those with even numbers represent blue-light-exposed coleoptiles. Proteins from cytosolic (1 and 2), Triton-sensitive (3 and 4), and SDS-sensitive (5 and 6) compartments were analyzed. Densitometric quantitation of the respective bands was performed with appropriate background subtractions, and the mean ± SD of five independent repeats of the experiment is plotted as a histogram on the right side. *Solid bars* indicate etiolated coleoptiles and open bars represent blue-light-exposed coleoptiles

localization of this protein onto the plasma membrane (Fig. 2Ed, Ef).

Detection of NADPH Oxidase Activity

NADPH oxidase activity was quantitated as a function of the gain of superoxide production in wheat coleoptile homogenates in the presence of added quantities of NADPH. The results are summarized in Table 1. In etiolated coleoptiles, NADPH-dependent superoxide production could be observed in 2-, 4-, 6-, and 8-mm segments, and the activity was highest in the extreme tip. Blue light exposure brought about a 30-fold increase in the NADPH activity associated with the 2-mm segment, whereas the other segments tested did not show blue-light-dependent activation of this enzyme.

Treatment with DPIC and staurosporine brought about highly significant ($P < 0.001$) inhibition of the generation of $O_2^{\cdot-}$ in blue-light-illuminated coleoptile tip homogenates. The basal level of superoxide production observed in 4-, 6-, and 8-mm segments was also inhibited by these reagents.

Histochemical Assay and Immunoblot Analysis of Superoxide Dismutase

An etiolated coleoptile tip showed no achromatic zone signifying SOD activity at the tip (Fig. 3a), and a corresponding control prepared by inhibiting SOD by DDC did not show any difference (Fig. 3b). However, a clear achromatic zone representing areas rich in SOD activity was visible in the case of blue-light-exposed coleoptile tips (Fig. 3c). Control sections treated with DDC as a SOD inhibitor brought about the loss of the achromatic zone (Fig. 3d), confirming that the achromatic zone appeared due to SOD activity. Thus, the histochemical assay for SOD showed heavy localization of the enzyme on the whole coleoptile tissue. Immunoblotting with anti-CuZn-SOD antibody detected a 20-kDa band predominantly present in cytosolic fractions (Fig. 3e, lanes 1 and 2) and weakly in the membrane fractions (Fig. 3e, lanes 3 and 4). The levels of cytosolic SOD showed a twofold increase upon blue light exposure (Fig. 3e, lane 2). MnSOD was detected in traces in cytosolic fractions from etiolated (Fig. 3f, lane 1) and blue-light-exposed (Fig. 3f, lane 2)

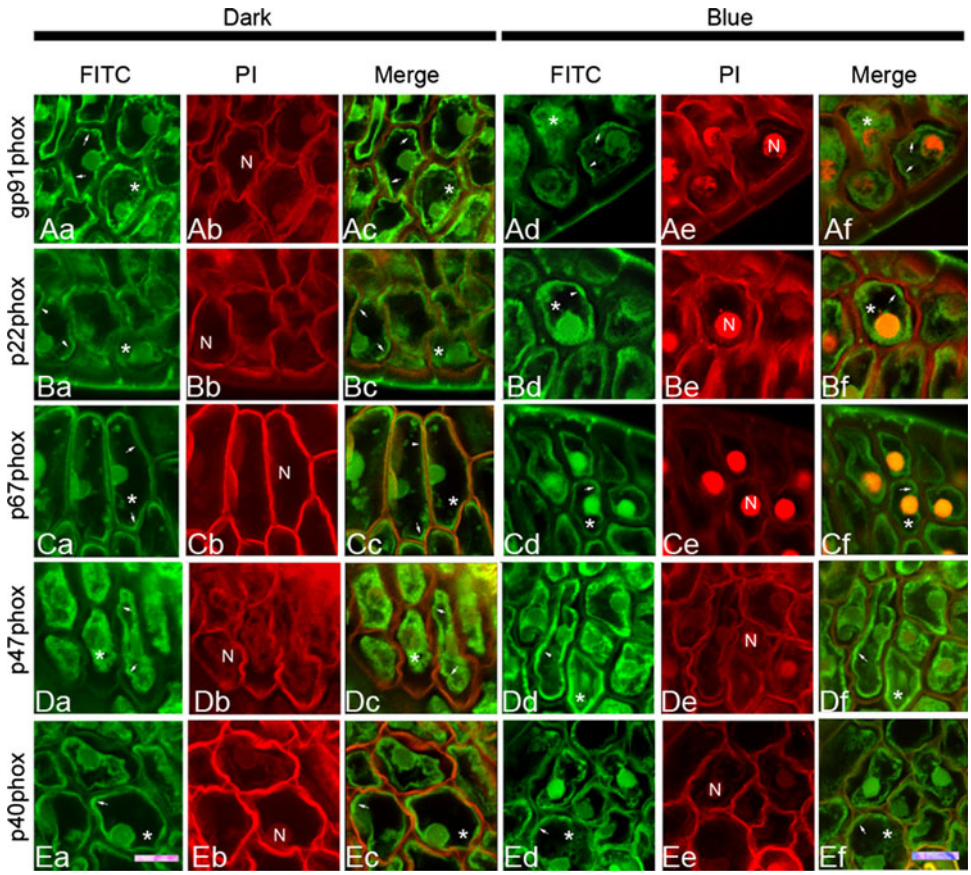

Fig. 2 Confocal images of optical sections of dark and blue-light-illuminated coleoptile tips probed with gp91phox (**A**a–**A**f), p22phox (**B**a–**B**f), p67phox (**C**a–**C**f), p47phox (**D**a–**D**f), and p40phox (**E**a–**E**f) antibodies. Anti-rabbit IgG raised in goat was used as a secondary antibody and PI was used for nuclear staining. FITC fluorescence was acquired in the green channel, PI fluorescence in the red channel, and merged images are presented in columns labeled accordingly. The plasma membrane is marked by *solid white arrows*, cytoplasm with *asterisks*, and nucleus with the *letter N*. Note the nuclear translocation of gp 91, p22, p67, and p47 NOX subunits. The experiments were repeated five times and representative images are included in this figure. Scale bar = 35 μM

Table 1 NADPH oxidase activity in wheat coleoptiles

Treatment	NADPH oxidase activity			
	2 mm	4 mm	6 mm	8 mm
Dark	21.4 ± 1.2	15 ± 2.01	13 ± 3.20	13 ± 2.96
Blue	643.0 ± 7.3*	18 ± 2.57	16 ± 5.33	15 ± 2.44
Blue + DPIC	8.1 ± 1.1**	3.17 ± 0.05	3.54 ± 0.98	4.08 ± 0.03
Blue + staurosporine	4.5 ± 1.3**	ND	ND	ND

Values indicate the amount of NADPH oxidized, expressed as nmol/min/mg of protein. All values are mean ± SD of five replicates analyzed
* $P < 0.001$ when compared with the dark control; ** $P < 0.001$ when compared with the blue-light-treated samples

coleoptiles. However, there was a highly significant increase in MnSOD levels in Triton X-100 extracts of blue-light-exposed coleoptiles (Fig. 3f, lane 4) compared to etiolated controls (Fig. 3f, lane 3).

Effect of NADPH Oxidase Inhibitors on Superoxide Anion Generation and Phototropic Curvature

In vivo profiling of active oxygen species in wheat coleoptile tip was monitored by the FDA fluorescence studies. Blue-light-illuminated coleoptile exhibited intense FDA fluorescence in the extreme tip (Fig. 4b), indicating the generation of H_2O_2, compared to the dark control (Fig. 4a). DPIC treatment followed by blue light illumination markedly reduced FDA fluorescence in the tip (Fig. 4c). Staurosporine also brought about a similar effect (Fig. 4d).

The effect of DPIC and staurosporine on phototropic curvature of coleoptiles was examined. Dark-grown coleoptiles showed no phototropic response (Fig. 4e), whereas unilateral blue light exposure resulted in visible phototropic curvature (Fig. 4f). Both NOX inhibitors used in this study quenched the blue-light-initiated ROS burst and could also abrogate the phototropic curvature in response to blue light exposure (Fig. 4g, h). The results are summarized in Table 2.

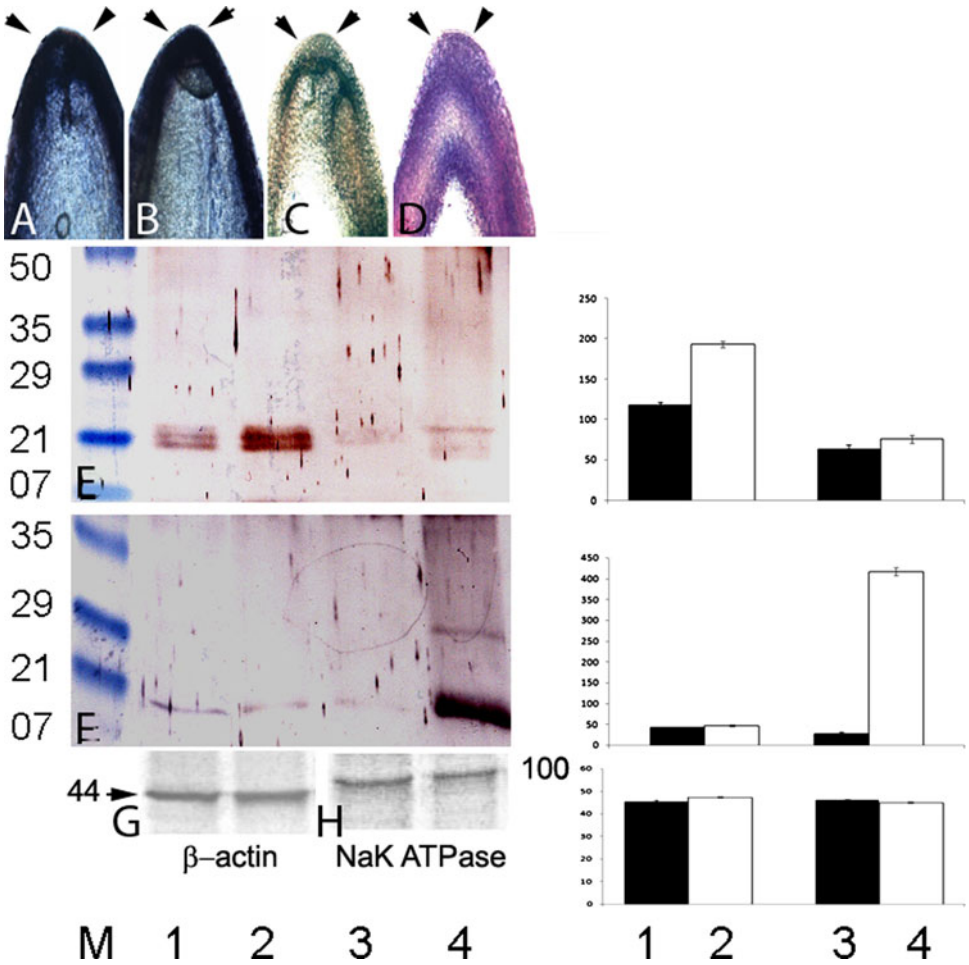

Fig. 3 Localization of SOD on wheat coleoptile tip. Longitudinal sections of etiolated and untreated coleoptile tips stained with NBT served as dark control (**a**), dark control sections treated with SOD inhibitor before color development (**b**), wheat coleoptile showing yellow discoloration due to oxidation of NBT by SOD in the presence blue light (**c**) when compared with (**d**), which represents SOD inhibitor-treated section that retained the color of NBT. Note the bleaching in (**c**) due to high SOD activity in the blue-light-illuminated section (region of interest is marked with *arrows*). Western blot analysis of CuZnSOD (**e**) and MnSOD (**f**) in coleoptiles. *β*-actin was used as loading control for cytosolic proteins (**g**) and NaK-ATPase for membrane proteins (**h**). Lanes 1 and 2 are of cytosolic proteins while lanes 3 and 4 are of membrane proteins. Dark (lanes 1 and 3) and blue-light-illuminated (lanes 2 and 4) were analyzed. M, molecular weight markers. Note the expression of CuZnSOD and MnSOD in blue-light-exposed coleoptiles. Histogram represents quantitative evaluation of the data from five independent replicates of the experiments. The data points represent mean ± SD

Discussion

NOX has been linked with oxidative burst in plants in response to a host of stimuli (Apostol and others 1989; Auh and Murphy 1995; Tenhaken and others 1995; Desikan and others 1996; Doke and others 1996; Keller and others 1998; Laloraya and others 1999; Sagi and Fluhr 2001; Chandrakuntal and others 2004). Activation of NOX requires the translocation of its cytosolic subunits, that is, p40phox, p47phox, and p67phox, toward the membrane-associated cytochrome-b558, composed of gp91phox and p22phox. This assembly process involves a Ca^{2+}-dependent protein kinase that catalyzes the phosphorylation of p67phox and p47phox, facilitating their translocation to the plasma membrane in plants (Xing and others 1997). Interestingly, antibodies raised against human gp91phox, p22phox, p47phox, and p67phox cross-reacted with appropriately similarly sized polypeptides in plant extracts (Tenhaken and others 1995; Desikan and others 1996; Keller and others 1998). The present study indicated the presence of NOX subunits in wheat coleoptiles that could cross-react with antibodies to neutrophil NOX antibodies (Fig. 1).

Blue light exposure of the coleoptile tips resulted in increased expression of p22phox, p67phox, p47phox, and p40phox, whereas gp91phox levels were not affected (Fig. 1). Blue light also brought about an increase in the association of p67phox and p40phox to the plasma membrane, and the association appeared to be strong because it could not be destabilized by Triton X-100 (Fig. 1).

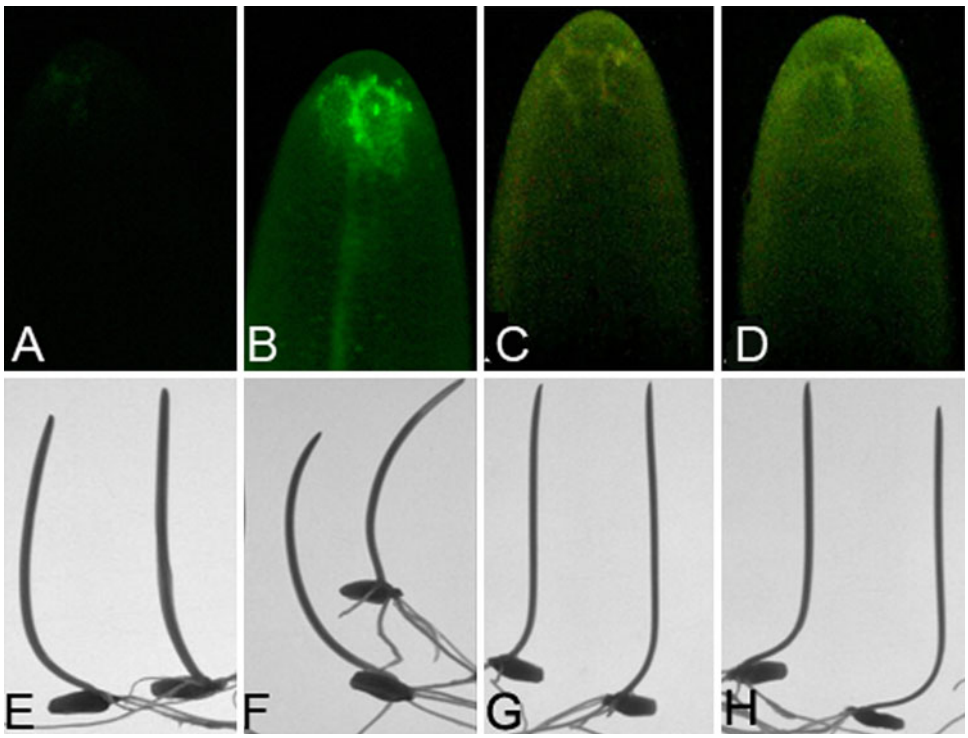

Fig. 4 Detection of superoxide radical in the coleoptile tip. Dark-grown coleoptile showing (**a**) no fluorescence and (**b**) FDA fluorescence in blue-light-illuminated tip. In vivo quenching effect of DPIC (**c**) and staurosporine (**d**) on blue-light-mediated generation of active oxygen species. Etiolated coleoptiles showing no curvature (**e**) and blue-light-exposed coleoptiles showing clear phototropic curvature (**f**) are shown. Coleoptile treated with DPIC (**g**) and staurosporine (**h**) showed marked inhibition in phototropic curvature. The data are representative of observations from five independent replicates

Table 2 Effect of DPIC and staurosporine on growth and phototropic curvature in wheat coleoptiles

Treatment	Coleoptile length (cm)	Coleoptile curvature (deg)
Dark	5.36 ± 1.28	ND
Dark + DPIC	5.02 ± 0.05	ND
Dark + staurosporine	5.11 ± 1.93	ND
Blue	5.16 ± 1.28	36.57 ± 13.74
Blue + DPIC	6.0 ± 1.29	5.00 ± 4.47*
Blue + staurosporine	6.11 ± 1.03	4.57 ± 4.23*

All values are mean ± SD of five replicates analyzed

* $P < 0.001$ when compared with the blue-light-treated samples

ND not detected

p47phox associated with the plasma membrane in a Triton X-100-sensititve fashion in blue-light-exposed coleoptiles. Thus, there is a clear indication of enhanced *de novo* expression of Nox components and their partitioning in coleoptile cells in response to blue light. Localization of gp91phox, p22phox, and p67phox on the nuclear membrane and within the nucleus is a novel observation (Fig. 2). Nox4 has been shown to localize to the nucleus of human umbilical vein endothelial cells (Kuroda and others 2005). Even though the nuclear localization of the NOX family oxidases has been suggested in several types of cells (Ushio-Fukai 2006), this observation of the dual targeting of NOX components by blue light is the first report in any plant system. Blue-light-induced nuclear translocation of NOX subunits supports a recent argument about nuclear superoxide production, which may have implications in chromatin remodeling and associated transcriptional regulations. The presence of active SOD in the photoreceptive part of the coleoptile tip explains the generation of H_2O_2 in apical zones that constitutes the major translocating active oxygen species involved in the blue light signal transduction (Chandrakuntal and others 2004).

Blue light excitation of the photoreceptor in the presence of NADPH reduces molecular oxygen to the superoxide radical (Laloraya and others 1999). This is mediated by a plasma membrane oxidase similar to the NADPH oxidase complex in the plasma membrane of mammalian phagocytes (Doke and others 1996), which catalyzes the one-electron reduction of molecular oxygen to $O_2^{\cdot-}$. Rapid dismutation of $O_2^{\cdot-}$ to H_2O_2 enhances light-mediated phosphorylation by activating kinase action in animals (Aitken and others 1995) and in plants (Reymond and others 1992; Sharma and others 1997). The initial photochemistry underlying cryptochrome function and regulation is its phosphorylation (Shalitin and others 2003; Ozgur and Sancar 2006; Immeln and others 2007; Inoue and others 2008). Though cryptochromes are autophosphorylated by the activity of a C-terminal kinase domain, a Chlamydomonas cryptochrome CPH1 lacking the C-terminal domain exhibited light-dependent phosphorylation, suggesting that the C terminus is dispensable for

autophosphorylation (Immeln and others 2007). Considering the sensitivity of the phototropic response to DPIC, it is reasonable to suspect that the $O_2^{\cdot-}$ and H_2O_2 generated through a Nox-dependent pathway might be involved in the phosphorylation of cryptochrome. Conversely, the downstream effects of cryptochrome activation also include ROS production (Danon and others 2006; Solov'yov and Schulten 2009). ROS can also act as redox signals that modulate the activity of target proteins through the reversible oxidation of critical protein thiols, thus altering the activity of enzymes, kinases, phosphatases, and transcription factors in mitochondria, the cytosol, or the nucleus (Murphy 2009). Although ROS production in the cytosol, mitochondria, and on the plasma membrane is well accepted, the recent demonstration of the presence of Nox4 and associated NADPH oxidase activity in the nucleus of human vascular endothelial cells indicated the possibility of nuclear oxidative stress response regulating gene expression (Kuroda and others 2005).

We demonstrated here that DPIC and staurosporine treatment of coleoptiles prior to blue light exposure resulted in heavy inhibition of superoxide production, supporting the notion of its NADPH oxidase dependence. Very low concentrations of DPIC inhibit NADPH oxidase by binding to its flavoprotein (Cross and Jones 1986). The inhibition of $O_2^{\cdot-}$ radical generation by DPIC clearly points to the involvement of NADPH oxidase in triggering the blue-light-induced signal transduction.

In the present study we report on the characterization of a NOX system in wheat coleoptile and its activation and dual targeting upon blue light exposure. We conclude that blue light signal cascades in the coleoptile tip are initialized and maintained by NOX-mediated generation of active oxygen species and is subsequently dismutated to H_2O_2 by the colocalized CuZnSOD, which further acts as a second messenger. The observed inhibitory effect of DPIC and staurosporine on NOX and the subsequent quenching of free radicals support this view. Thus, this study reports for the first time that blue light activates NOX in wheat coleoptile tips, triggering the reactive oxygen burst by a two-pronged trafficking of cytosolic NOX components, targeting the nuclear membrane and plasma membrane which initiates molecular events leading to the phototropic response. Evaluating the phototropic response in suitable NOX-deficient mutants would be required to further confirm the role of NOX in blue light signaling in coleoptiles.

Acknowledgments This work was supported through Grant No. SP/SO/A-10/2000 to MML. KCK received a Senior Research Fellowship from the Council of Scientific and Industrial Research V. Jiji provided technical help with confocal laser scan microscopy. ESR studies were conducted at the School of Life Sciences, Devi Ahilya University, Indore. The authors thank J. Khurana for technical discussions.

References

Aitken RJ, Paterson M, Fisher H, Buckingham DW, van Duin M (1995) Redox regulation of tyrosine phosphorylation in human spermatozoa and its role in the control of human sperm function. J Cell Sci 108(Pt 5):2017–2025

Apostol I, Heinstein PF, Low PS (1989) Rapid stimulation of an oxidative burst during elicitation of cultured plant cells: role in defense and signal transduction. Plant Physiol 90:109–116

Auh CK, Murphy TM (1995) Plasma membrane redox enzyme is involved in the synthesis of $O_2^{\cdot-}$ and H_2O_2 by phytophthora elicitor-stimulated rose cells. Plant Physiol 107:1241–1247

Babourina O, Godfrey L, Voltchanskii K (2004) Changes in ion fluxes during phototropic bending of etiolated oat coleoptiles. Ann Bot (Lond) 94:187–194

Bedard K, Lardy B, Krause KH (2007) NOX family NADPH oxidases: not just in mammals. Biochimie 89:1107–1112

Bokoch GM (1994) Regulation of the human neutrophil NADPH oxidase by the Rac GTP-binding proteins. Curr Opin Cell Biol 6:212–218

Briggs WR, Christie JM, Salomon M (2001) Phototropins: a new family of flavin-binding blue light receptors in plants. Antioxid Redox Signal 3:775–788

Brown DI, Griendling KK (2009) Nox proteins in signal transduction. Free Radic Biol Med 47:1239–1253

Chandrakuntal K, Kumar PG, Laloraya M, Laloraya MM (2004) Direct involvement of hydrogen peroxide in curvature of wheat coleoptile in blue-light-treated and dark-grown coleoptiles. Biochem Biophys Res Commun 319:1190–1196

Cross AR, Jones OT (1986) The effect of the inhibitor diphenylene iodonium on the superoxide-generating system of neutrophils. Specific labelling of a component polypeptide of the oxidase. Biochem J 237:111–116

Danon A, Coll NS, Apel K (2006) Cryptochrome-1-dependent execution of programmed cell death induced by singlet oxygen in *Arabidopsis thaliana*. Proc Natl Acad Sci USA 103:17036–17041

Desikan R, Hancock JT, Coffey MJ, Neill SJ (1996) Generation of active oxygen in elicited cells of *Arabidopsis thaliana* is mediated by a NADPH oxidase-like enzyme. FEBS Lett 382:213–217

Doke N, Miura Y, Sanchez LM, Park HJ, Noritake T, Yoshioka H, Kawakita K (1996) The oxidative burst protects plants against pathogen attack: mechanism and role as an emergency signal for plant bio-defence—a review. Gene 179:45–51

Foreman J, Demidchik V, Bothwell JH, Mylona P, Miedema H, Torres MA, Linstead P, Costa S, Brownlee C, Jones JD, Davies JM, Dolan L (2003) Reactive oxygen species produced by NADPH oxidase regulate plant cell growth. Nature 422:442–446

Immeln D, Schlesinger R, Heberle J, Kottke T (2007) Blue light induces radical formation and autophosphorylation in the light-sensitive domain of Chlamydomonas cryptochrome. J Biol Chem 282:21720–21728

Inoue S, Kinoshita T, Matsumoto M, Nakayama KI, Doi M, Shimazaki K (2008) Blue light-induced autophosphorylation of phototropin is a primary step for signaling. Proc Natl Acad Sci USA 105:5626–5631

Kay CW, Schleicher E, Kuppig A, Hofner H, Rudiger W, Schleicher M, Fischer M, Bacher A, Weber S, Richter G (2003) Blue light perception in plants. Detection and characterization of a light-induced neutral flavin radical in a C450A mutant of phototropin. J Biol Chem 278:10973–10982

Keller T, Damude HG, Werner D, Doerner P, Dixon RA, Lamb C (1998) A plant homolog of the neutrophil NADPH oxidase

gp91phox subunit gene encodes a plasma membrane protein with Ca^{2+} binding motifs. Plant Cell 10:255–266

Kuroda J, Nakagawa K, Yamasaki T, Nakamura K, Takeya R, Kuribayashi F, Imajoh-Ohmi S, Igarashi K, Shibata Y, Sueishi K, Sumimoto H (2005) The superoxide-producing NAD(P)H oxidase Nox4 in the nucleus of human vascular endothelial cells. Genes Cells 10:1139–1151

Laloraya MM, Chandrakuntal K, Kumar GP, Laloraya M (1999) Active oxygen species in blue light mediated signal transduction in coleoptile tips. Biochem Biophys Res Commun 256:293–298

Murphy MP (2009) How mitochondria produce reactive oxygen species. Biochem J 417:1–13

Ozgur S, Sancar A (2006) Analysis of autophosphorylating kinase activities of *Arabidopsis* and human cryptochromes. Biochemistry 45:13369–13374

Reymond P, Short TW, Briggs WR (1992) Blue light activates a specific protein kinase in higher plants. Plant Physiol 100: 655–661

Sagi M, Fluhr R (2001) Superoxide production by plant homologues of the gp91(phox) NADPH oxidase. Modulation of activity by calcium and by tobacco mosaic virus infection. Plant Physiol 126:1281–1290

Shalitin D, Yang H, Mockler TC, Maymon M, Guo H, Whitelam GC, Lin C (2002) Regulation of *Arabidopsis* cryptochrome 2 by blue-light-dependent phosphorylation. Nature 417:763–767

Shalitin D, Yu X, Maymon M, Mockler T, Lin C (2003) Blue light-dependent in vivo and in vitro phosphorylation of *Arabidopsis* cryptochrome 1. Plant Cell 15:2421–2429

Sharma VK, Jain PK, Maheshwari SC, Khurana JK (1997) Rapid blue light induced phosphorylation of plasma-membrane-associated proteins in wheat. Phytochem 44:775–780

Solov'yov IA, Schulten K (2009) Magnetoreception through cryptochrome may involve superoxide. Biophys J 96:4804–4813

Taylor WR, Jones DT, Segal AW (1993) A structural model for the nucleotide binding domains of the flavocytochrome b-245 beta-chain. Protein Sci 2:1675–1685

Tenhaken R, Levine A, Brisson LF, Dixon RA, Lamb C (1995) Function of the oxidative burst in hypersensitive disease resistance. Proc Natl Acad Sci USA 92:4158–4163

Ushio-Fukai M (2006) Localizing NADPH oxidase-derived ROS. Sci STKE 2006:re8

Xing T, Higgins VJ, Blumwald E (1997) Race-specific elicitors of *Cladosporium fulvum* promote translocation of cytosolic components of NADPH oxidase to the plasma membrane of tomato cells. Plant Cell 9:249–259